Chemical Engineering Journal 395 (2020) 125114

Contents lists available at ScienceDirect

Chemical Engineering Journal

journal homepage: www.elsevier.com/locate/cej

# Melamine N-oxide based self-assembled energetic materials with balanced energy & sensitivity and enhanced combustion behavior

Siwei Song[a], Yi Wang[a,*], Wei He[b], Kangcai Wang[a], Mi Yan[a], Qilong Yan[b], Qinghua Zhang[a,*]

[a] *Institute of Chemical Material, China Academy of Engineering Physics, Mianyang 621000, China*
[b] *Science and Technology on Combustion, Internal Flow and Thermostructure Laboratory, Northwestern Polytechnical University, Xi'an 710072, China*

## HIGHLIGHTS

- Assembling fuel explosives with oxidants for developing novel energetic materials.
- A novel fuel-rich explosive TTDO was designed and synthesized.
- TTDOP showed good energy & safety balance and enhanced combustion behavior.

## GRAPHICAL ABSTRACT

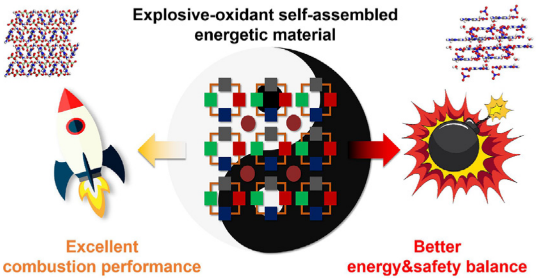

## ARTICLE INFO

*Keywords:*
Energetic materials
High-energy oxidants
Intermolecular assembly
Detonation property
Low sensitivity
Combustion behavior

## ABSTRACT

Development of advanced energetic materials with promising properties has been intensely-pursued over the past decades. However, traditional strategies for integrating fuel skeleton and oxidizing groups into an organic molecule are very difficult to balance the contradictory relationship between high energy and low sensitivity of energetic materials. In this work, we present a promising approach to develop advanced energetic materials through intermolecular assembly of nitrogen-rich triazine energetic compounds and high-energy oxidants. Under the direction of electrostatic potential and proton affinity calculations, a novel energetic compound 2,4,6-triamino-1,3,5-triazine-1,3-dioxide (TTDO) was rationally designed and synthesized. The easy and effective self-assembly of TTDO with high-energy oxidants afforded a series of novel advanced energetic materials with a good balance between energy and sensitivity. Among these self-assembled energetic materials, TTDOP (a self-assembled energetic material between TTDO and $HClO_4$) showed a very high density (2.047 g $cm^{-3}$ at 100 K), detonation properties (9284 m $s^{-1}$ and 41 GPa) as high as that of HMX and better mechanical sensitivity (13 J and 144 N). Moreover, TTDOP exhibited great promise as a substitute for ammonium perchlorate (AP) in solid propellant formulations due to its high combustion and propulsion performances. This work opens a new avenue to develop intermolecular energetic materials with well balanced energy & sensitivity and versatile functionality.

## 1. Introduction

Energetic materials are a class of special reactive substances with high amounts of stored chemical energy, which include high explosives, propellants and pyrotechnics [1,2]. In the development of human society, energetic materials have provided immense impetus to remake nature, especially in the field of engineering construction and space propulsion [3–6]. As the development of this material subject with long

---

* Corresponding authors.
*E-mail addresses:* ywang0521@caep.cn (Y. Wang), qinghuazhang@caep.cn (Q. Zhang).

https://doi.org/10.1016/j.cej.2020.125114
Received 22 January 2020; Received in revised form 13 March 2020; Accepted 15 April 2020

history, the era of pursuing superior single performance (like explosive applications) has passed. Compared with typical high explosives like cyclotrimethylenetrinitramine (RDX), cyclotetramethylenetetranitramine (HMX) and solid propellant oxidizers ammonium perchlorate (AP) and ammonium dinitramide (ADN), modern advanced energetic materials should meet more strict requirements and meanwhile have excellent comprehensive performances including high-energy, low-sensitivity, and functional versatility, etc [7,8]. Thus, it is highly desirable to explore new design strategies for the development of advanced energetic materials.

Due to the intrinsic need of rapid self-sustained redox exothermic decomposition reaction, the development of new advanced energetic materials can be understood as an integration process of fuel and oxidant components via intramolecular or intermolecular ways [9]. In general, intramolecular integration of fuel (e.g., carbon skeleton and amino group) and oxidizing organic groups (e.g., $-NO_2$, $-ONO_2$, etc.) within a molecular scaffold is the primary choice, because this method can generate a certain molecule with precise element composition, crystal structure and its easily addressed structure-property relationship. For these one-component energetic materials, however, it is difficult to achieve a good energy-safety balance owing to the close linking of fuel and oxidizing groups in a single molecule. Moreover, with the ascertained element composition and molecular structure, these energetic materials usually exhibit poor adjustability in their energy levels with an obvious energy limit (Fig. 1a). As an alternative method, intermolecular self-assembly strategy of integrating fuel and oxidant molecule into an energetic system has attracted increasing interest in the development of advanced energetic materials. A typical example is the metastable intermixed composites (MICs), an important kind of nanometre scaled intermolecular fuel-oxidant mixtures, which are widely studied and used for combustion applications (Fig. 1b) [10]. Very recently, energetic molecular perovskites and oxidant-loaded porous energetic materials (such as MOFs and ZIFs) were also developed as novel intermolecular integrated energetic systems [11,12]. Nevertheless, the fuel parts in them are non-energetic components (e.g., 1,4-diazabicyclo[2.2.2]octane for energetic molecular perovskites and 1,4-benzenedicarboxylate for oxidant-loaded MOFs), resulting in their relatively low oxygen balances (OB) and thereby undesired detonation performances (Fig. 1c) [13].

For some traditional high explosives, although they are designed through intramolecular combination of fuel and oxidizing moieties within a molecular scaffold, they are also capable of further assembling oxidant molecules to fabricate new intermolecular energetic systems [14,15]. This novel strategy of assembling explosive and oxidant molecules in an energetic system can help to overcome the energy limit of traditional high explosives and as a consequence facilitate to accelerate

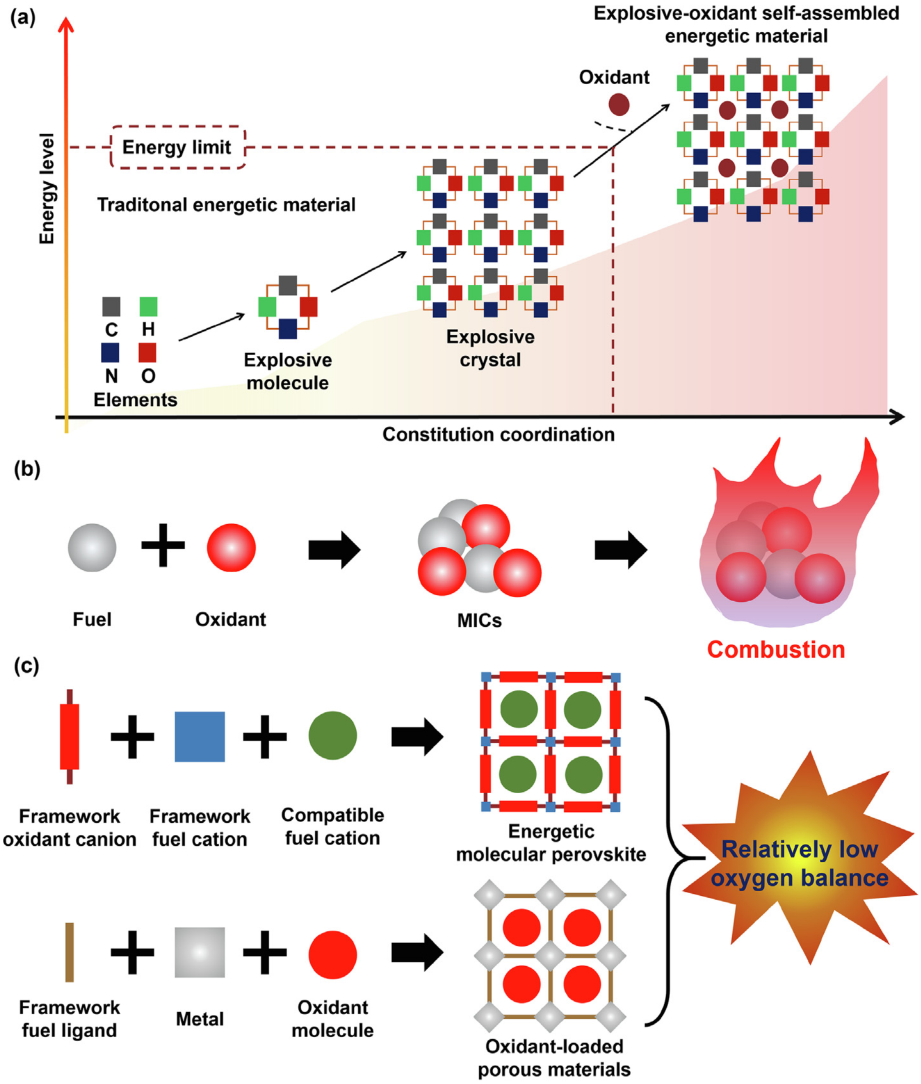

**Fig. 1.** (a) Illustration of explosive-oxidant self-assembled strategy and its comparison with traditional energetic material. (b) Schematic of metastable intermixed composites. (c) Schematic of energetic molecular perovskite and oxidant-loaded porous materials.

the discovery of novel multifunctional energetic materials (Fig. 1a). With this consideration, very recently we developed three advanced energetic materials through self-assembly of 2,4,6-triamino-5-nitropyrimidine 1,3-dioxide (ICM-102) and different oxidants with the aid of non-covalent interactions [16,17]. These self-assembled energetic materials exhibit good energy-safety balance and combustion behavior. For the explosive precursor of ICM-102, however, its capability of assembling different oxidants is relatively limited, and the experimental studies demonstrate that only one N-oxide group in the structure can be utilized to combine the oxidants. Here, we designed and synthesized a novel explosive precursor with relatively higher proton affinity, 2,4,6-triamino-1,3,5-triazine-1,3-dioxide (TTDO), which is an analogue of ICM-102 and also has two N-oxide bonds in its molecular structure. As expected, two N-oxide bonds of TTDO are capable of combining more than one oxidant molecules to form new self-assembled energetic materials, e.g., the ratios of TTDO and three oxidants ($H_2O_2$, $HNO_3$ and $HClO_4$) in the crystals of three self-assembled energetic materials are 1:1.75, 1:2 and 1:2, respectively. As a result, the density of assembled energetic material 2,4,6-triamino-1,3,5-triazine-1,3-dioxide-$HClO_4$ (TTDOP) is as high as 1.988 g $cm^{-3}$ at room temperature (2.047 g $cm^{-3}$ at 100 K). The detonation properties (9284 m $s^{-1}$ and 41 GPa) of TTDOP is comparable to that (9235 m $s^{-1}$ and 38.9 GPa) of HMX, while its impact sensitivity (13 J) is close to that (impact sensitivity: 15 J) of TNT (2,4,6-trinitrotoluene). Moreover, the combustion and propulsion properties reveal that TTDOP may also has potential application in solid propellant. This work also demonstrated the universality of the explosive-oxidant self-assembled strategy for the development of advanced energetic materials.

## 2. Experimental section

### 2.1. General

Reagents were purchased from commercial resources and were used without further purification. $^{13}C$ spectra were collected on a Bruker Avance Neo 400 NMR spectrometer operating at 100 MHz, respectively. X-Ray single-crystal diffraction data were collected on an Oxford Xcalibur3 diffractometer with MoKα radiation (λ = 0.71073 Å). Impact and friction sensitivity measurements were made using a standard BAM Fall hammer and a BAM friction tester. Combustion test were launched by a self-built test platform with a high speed camera operating at 1 kHz.

### 2.2. Synthesis

#### 2.2.1. TTDO (2,4,6-triamino-1,3,5-triazine-1,3-dioxide)

Melamine (12.6 g, 100 mmol) is completely dissolved in trifluoroacetic acid (130 ml) at 50 °C to give a clear solution, then 30% hydrogen peroxide (12 ml) was added dropwise into the above solution. After stirring for 6 h, white precipitates formed and were filtered out. The precipitates then completely dissolved in water and were neutralized to pH = 7 to give new white precipitates. After filtration and drying, white sample of TTDO was obtained at a yield of 51%. TTDO is difficult to be dissolved in organic solvents like DMSO and was slightly soluble in water, thus only its $^{13}C$ were recorded as: $^{13}C$ NMR ($D_2O$, 100 MHz) δ: 151.904, 150.776 ppm. The crystallographic data and $^{13}C$ spectra for TTDO was provided in Supporting Information (see Table S1 and Fig. S5).

#### 2.2.2. TTDOH (2,4,6-triamino-1,3,5-triazine-1,3-dioxide-$H_2O_2$ self-assembled energetic material)

0.2 g TTDO was suspended in 10 ml 30% $H_2O_2$ aqueous solution and then the mixture was filtered to give a saturated solution. After slow solvent evaporation at 30 °C in drying oven for several days, colorless crystals (named as TTDOH) suitable for single-crystal X-ray diffraction analysis were collected at a yield of 80%.

#### 2.2.3. TTDON (2,4,6-triamino-1,3,5-triazine-1,3-dioxide-$HNO_3$ self-assembled energetic material)

1 g TTDO was dissolved in 2 ml white fuming nitric acid (WFNA). After evaporation in ambient condition for several hours, colorless crystals (named as TTDON) suitable for single-crystal X-ray diffraction analysis were collected at a yield of 40%.

#### 2.2.4. TTDOP (2,4,6-triamino-1,3,5-triazine-1,3-dioxide-$HClO_4$ self-assembled energetic material)

1 g TTDO was completely dissolved in 12 ml 70% perchloric acid ($HClO_4$) aqueous heated to 70 °C under stirring. Once the solution turned into clear, the stirring and heating was shut down to cooling crystallization. After half an hour, colorless crystals (named as TTDOP) suitable for single-crystal X-ray diffraction analysis could be obtained after filtration at a yield 54%.

## 3. Results and discussions

With the aims of designing and screening new explosive precursors with a good capacity of capturing oxidants, we first used the surface electrostatic potential (ESP) as an effective tool for interpreting and predicting the reactive behavior of molecules with high proton-affinity [18–21]. We particularly calculated and compared the ESPs of ICM-102 and its two analogues (i.e., 2,4,6-triaminopyrimidine-3,5-dioxide, TPDO and 2,4,6-triamino-1,3,5-triazine-1,3-dioxide, TTDO). As shown in Fig. 2a, the surface minimum points of three compounds are all located on their N-oxide bonds with the values of −31.7 kcal $mol^{-1}$, −35.0 kcal $mol^{-1}$ and −38.8 kcal $mol^{-1}$, respectively, which clearly indicates that the N-oxide bond is the first site to accept proton. In addition, we further calculated the ESPs of monoprotonated ICM-102, TPDO and TTDO, respectively (Fig. 2a). Because these molecules possessed one positive charge after protonation, all ESPs were positive (all the surfaces were red). The minimum of ESP on ICM-102 (36.6 kcal $mol^{-1}$) transferred to the area close to the nitro group, which well explained why N-oxides of ICM-102 could not be doubly protonated to capture two oxidant molecules. In contrast, minimum values of ESP on TPDO (31.7 kcal $mol^{-1}$) and TTDO (31.0 kcal $mol^{-1}$) were still close to N-oxide, enabling a possibility to be doubly protonated for TPDO and TTDO. Next, we directly calculated and compared the proton affinity of ICM-102 and TTDO (Fig. 2b) [22]. For the two steps of protonation, the proton affinities of TTDO are 9.51 eV and 5.74 eV, respectively, which are both higher than those of ICM-102 (9.16 eV and 5.50 eV). Based on above analysis, we can clearly find that TTDO has the lower negative ESP and higher proton affinity than that of ICM-102 and could be expected to show higher capacity of capturing more oxidant molecules. Thus, in this study we concentrate on the synthesis and self-assembly behavior between TTDO and different oxidants ($H_2O_2$, $HNO_3$ and $HClO_4$) and further evaluate their thermal, energetic and combustion properties as advanced energetic materials. The calculation details about ESPs and proton affinities are described in the Supporting Information.

TTDO and its derived self-assembled energetic materials was readily prepared as described in above sections (Fig. 3a). Gram-scale TTDO was prepared by the N-oxidization reaction of melamine in $CF_3COOH/H_2O_2$ condition. TTDOH and TTDON were obtained by dissolving TTDO into 30% hydrogen peroxide or white fuming nitric acid (WFNA) then crystallized through solvent evaporation. To obtain TTDOP, the TTDO should be thoroughly dissolved in 70% perchloric acid heated to 70 °C.Then the solution was naturally cooled down to room temperature, and the desired products precipitated as the white clear crystals. The crystals of TTDOH, TTDON and TTDOP were directly collected for the single-crystal X-ray diffraction. The crystallographic data were recorded in Tables S2–S4 in Supporting Information.

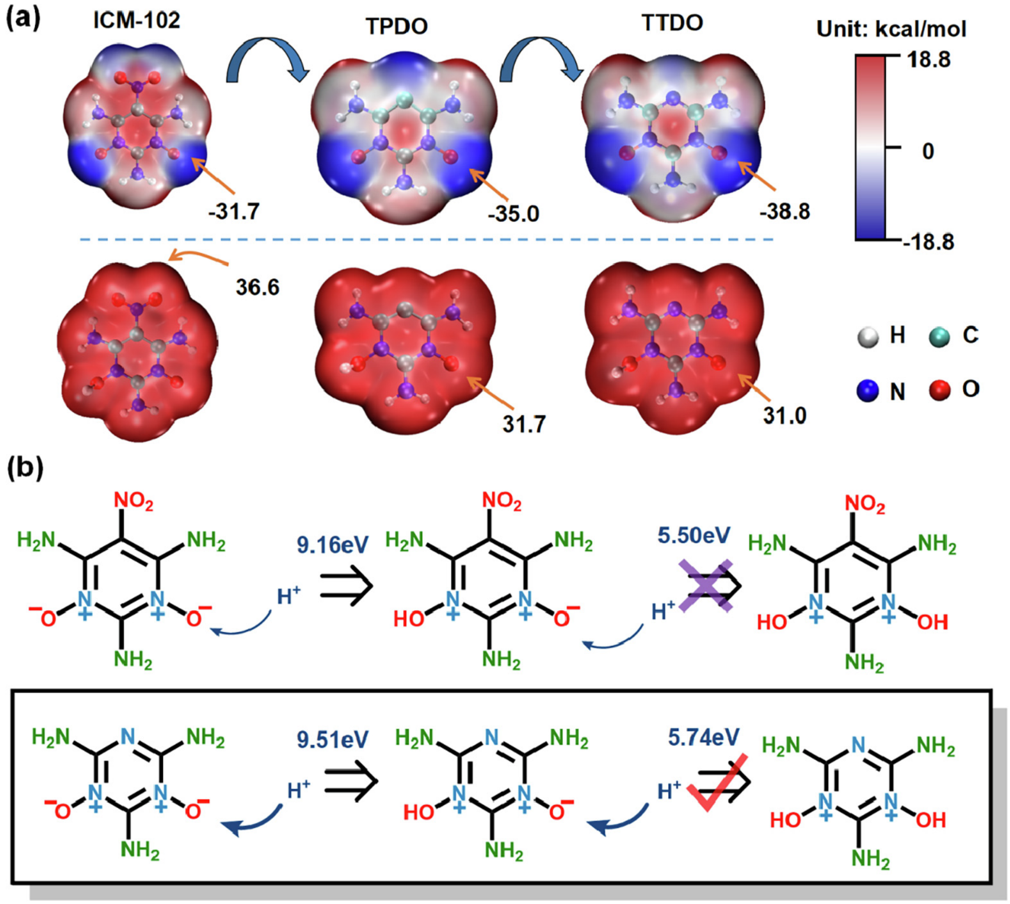

**Fig. 2.** (a) Electrostatic potential (at 0.001 a. u.) of ICM-102, TPDO and TTDO and their protonated derivatives. (b) Stepwise proton affinities for ICM-102 and TTDO.

### 3.1. Crystal structures

TTDOH crystallizes in triclinic space group P-1, whose asymmetric unit contains two TTDO molecules and three and a half hydrogen peroxide molecules with a crystal density of 1.754 g cm$^{-3}$ at 170 K (Fig. 3b). The crystal structure of TTDOH is cross-like framework (Fig. 3b left), which could be separated into two layered-like structures (layer distances are 3.173 Å and 2.956 Å, respectively) (Fig. 3b middle). One molecular layer is constructed by the supramolecular chains of TTDO dimers (the dimer is formed by the hydrogen bond between N-oxide and amino group with a length of 2.011 Å) and hydrogen peroxide dimers in an alternative arrangements (triple hydrogen bond exited with lengths of 2.016 Å, 2.253 Å and 2.037 Å). In the other layer, the identical dimers of TTDO (hydrogen bond length of 2.016 Å) is also observed but only one hydrogen peroxide molecule bridged the TTDO dimers to constructed a different supramolecular chain through hydrogen bond of 2.082 Å (Fig. 3b right). These supramolecular chains interwove with each other under the help of hydrogen bonds to give a complicated cross-like structure.

TTDON crystallizes in triclinic space group P-1 with a crystal density of 1.825 g cm$^{-3}$ at 175 K (Fig. 3c). The asymmetry unit of TTDON contains one doubly protonated TTDO molecule, two nitrate ions and one water molecule. Crystal packing of TTDON can be viewed as layer-like structure (Fig. 3c left). The supramolecular layer with cavities is constructed by protonated TTDO molecules, nitrate ions and water molecules. The nitrate ion in the layer has interactions with the adjacent protonated TTDO molecules through hydrogen bonds with length of 2.164 Å, 2.271 Å and 1.989 Å. Cavities in the supramolecular layer are occupied by the nitrate ions vertical to the layer (Fig. 3c right). These vertical nitrate ions are also constrained in the layer through two hydrogen binds with lengths of 2.092 Å and 2.068 Å. The steric effect due to intercalation of nitrate ions weaken the π-π interaction between layers and thus leads to a larger layer distance of 3.242 Å compared with the layers in TTDOH (Fig. 3c middle).

TTDOP crystallizes in monoclinic space group P 21/n with a crystal density of 2.047 g cm$^{-3}$ at 100 K (Fig. 3d). The asymmetry unit of TTDOP contains one doubly protonated TTDO molecule and two perchlorate anions. The perchlorate anions and protonated TTDO molecules constitute a sandwich layer-like structure (Fig. 3d left). When the perchlorate ions are removed, the protonated TTDO molecules could be viewed as wave-like layered structure with a distance of 4.584 Å between layers (Fig. 3d middle). Because there are some cavities and no obvious hydrogen bonds in the wave-like layer structure, the intra-layer assembly of protonated TTDO molecules are relatively incompact. As a result, the perchlorate anions play an essential role in the formation of wave-like layer structure for TTDOP. The relatively incompact intra-layer assembly of protonated TTDO molecules and large interlamellar spacing finally result in the lowest packing coefficient of 0.745 for TTDOP among these three explosive-oxidant self-assembled energetic materials (0.754 for TTDOH and 0.768 for TTDON). Thus, the high density of TTDOP can be mainly attributed to the high content of oxygen and chlorine elements rather than high packing coefficient.

Apart from the hydrogen bonds discussed above, more complicated hydrogen bond networks are existed in the crystal structures of TTDOH, TTDON and TTDOP and their detailed information are summarized in Tables S5–S7.

### 3.2. Detonation property, mechanical sensitivity and thermal stability

In general, the most attractive properties for energetic materials are their energy levels including detonation velocity (defined as the speed at which a detonation wave propagates steadily in an explosive column)

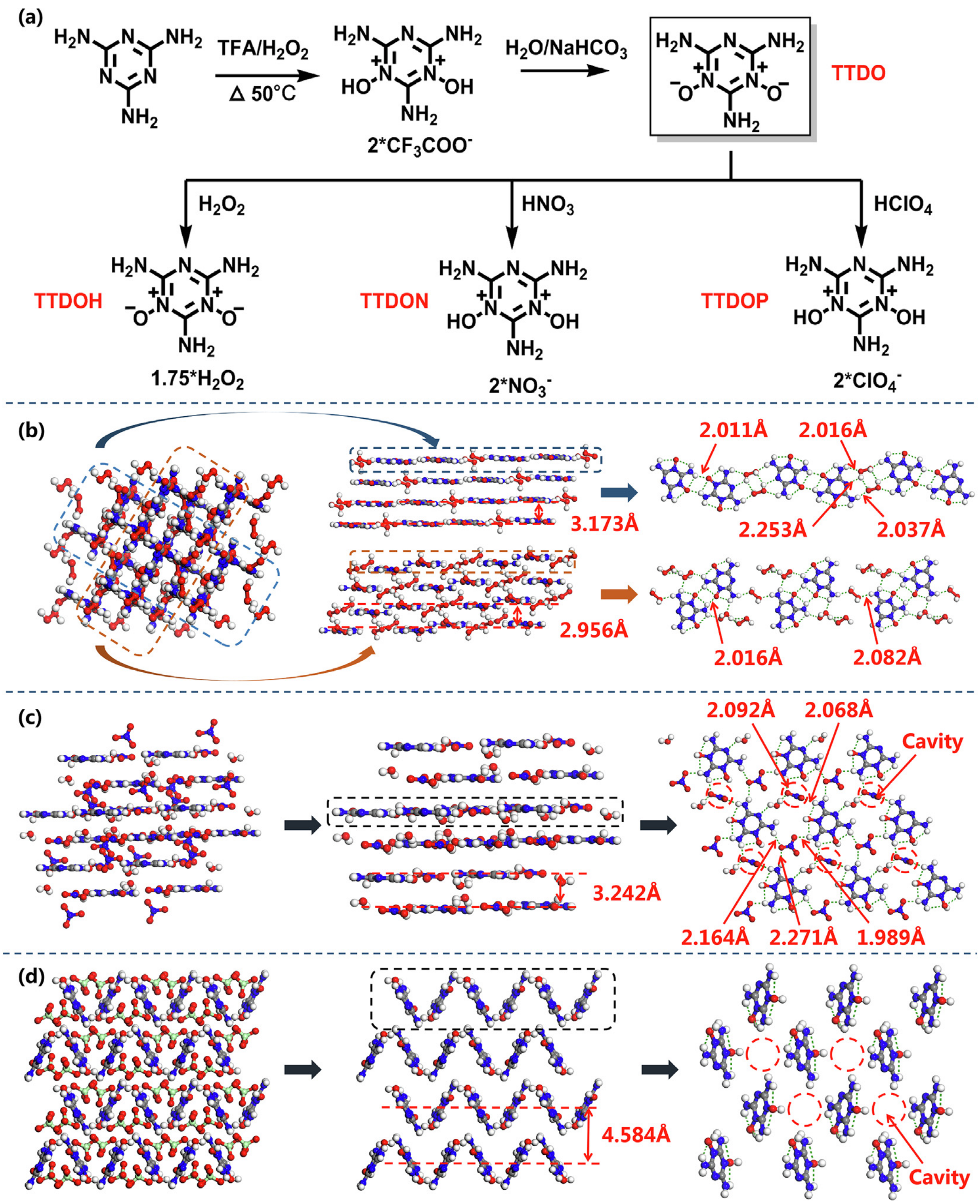

**Fig. 3.** (a) Synthesis routes of TTDO and the corresponding explosive-oxidant self-assembled energetic materials (TTDOH, TTDON and TTDOP). (b) 3D crystal structure and step-by-step enlarged view of TTDOH. (c) 3D crystal structure and step-by-step enlarged view of TTDON. (d) 3D crystal structure and step-by-step enlarged view of TTDOP.

and detonation pressure (defined as pressure on the detonation wave front when explosives explode) and mechanical sensitivities. The detonation properties that have a close correlations with heat of formation and density are also estimated by Explo5 (version 6.02) [23]. The heat of formation for the compounds were calculated by G4(MP2)_6x method [24] (more details were provided in Supporting information). Impact and friction sensitivity were tested experimentally by employing a standard BAM fall hammer and a BAM friction tester. All the property results are summarized in Table 1.

Despite no classical explosophores like nitro groups in the structure, TTDO has a higher $CO_2$-based OB (−70.9%), higher density (1.72 g $cm^{-3}$) and higher heat of formation (−6.41 kJ $mol^{-1}$) than those (−74%, 1.65 g $cm^{-3}$ and −67 kJ $mol^{-1}$) of TNT. Hence, the calculated detonation velocity and pressure (6924 m $s^{-1}$ and 20.7 GPa, respectively) of TTDO are very close to those of TNT (6881 m $s^{-1}$ and 19.5 GPa). When the oxidants were integrated into the crystal systems of TTDO, the OBs of self-assembled energetic materials are significantly increased. As a consequence, the detonation properties of three novel self-assembled energetic materials are significantly higher than those of TTDO. Among them, TTDOH possesses a relatively low detonation velocity of 8159 m $s^{-1}$ and a detonation pressure of 24.3 GPa, respectively, probably due to its low crystal density of 1.75 g $cm^{-3}$, negative heat of formation of −551.2 kJ $mol^{-1}$ and low $CO_2$-based OB (−38.6%). However, when compared with TNT (6924 m $s^{-1}$ and 20.7 GPa) , TTDOH has also demonstrated more desirable detonation performances (8159 m $s^{-1}$ and 24.3 GPa) but better mechanical sensitivity (> 20 J *vs* 15 J and > 360 N *vs* 353 N). With self-assembling TTDO with $HNO_3$ and $HClO_4$ respectively, the as-synthesized self-assembled

**Table 1**
Physicochemical properties.

| Cmpd | ρ (g cm$^{-3}$) | $\Delta_f H$[b] (kJ mol$^{-1}$) | OB[c] (%) | $D_v$[d] (m s$^{-1}$) | P[e] (GPa) | IS[f] (J) | $T_d$[j] (°C) |
|---|---|---|---|---|---|---|---|
| TTDO | 1.72[a] | −6.41 | −70.9 | 6924 | 20.7 | > 20 | 340 |
| TTDOH | 1.721/1.754(170 K)[b] | −551.2 | −38.6 | 8159 | 24.3 | > 20 | 311 |
| TTDON | 1.791/1.825(175 K)[b] | −31.5 | −11.3 | 8900 | 34.2 | 14 | 180 |
| TTDOP | 1.988/2.047(100 K)[b] | 714.2 | 4.5 | 9284 | 41.0 | 13 | 176 |
| TNT[i] | 1.650 | −67.0 | −74.0 | 6881 | 19.5 | 15 | 295 |
| RDX[i] | 1.806 | 70.3 | −21.6 | 8838 | 34.3 | 7.5 | 204 |
| HMX[i] | 1.905 | 116.1 | −21.6 | 9235 | 38.9 | 7.4 | 280 |
| AP[i] | 1.950 | −295.8 | 34.0 | 6368 | 15.8 | 15 | 350 |

[a] Density measured by gas pycnometer at room temperature. [b] Densities recalculated from low temperature single-crystal X-ray diffraction densities by the formula: $\rho_{298k} = \rho_T/[1 + 1.5 \times 10^{-4}(298 - T)]$. Values after slashes are measured densities at low temperature. [b] Calculated heat of formation in solid state. [c] Oxygen balance based on $CO_2$ for $C_aH_bN_cO_dCl_e$: $OB = 1600 \times [d - 2a - (b - e)/2]/M_w$. [d] Detonation velocity. [e] Detonation pressure. [f] Impact sensitivity. [g] Friction sensitivity. [h] Specific impulse. [i] Values from references [25,26]. [j] Decomposition temperature.

energetic materials, i.e., TTDON and TTDOP, displayed much higher densities, OBs and heats of formation than those of TTDOH. For TTDON, its detonation properties (8900 m s$^{-1}$ and 34.2 GPa) are close to those (8838 m s$^{-1}$ and 34.3 GPa) of RDX, but its mechanical sensitivities (14 J and 196 N) are much lower than those (7.5 J and 120 N) of RDX. More impressively, the detonation properties of TTDOP (9235 m s$^{-1}$ and 41GPa) is comparable to those (9235 m s$^{-1}$ and 38.9 GPa) of HMX with also better mechanical sensitivities (13 J *vs* 7.4 J and 144 N *vs* 120 N). Besides the spacial isolation of fuel (explosive) from oxidant, the absence of active explosophore groups (such as C-$NO_2$ and N-$NO_2$) may also contribute positively to the relatively low mechanical sensitivities for these self-assembled energetic materials [27].

To gain more insights into the intermolecular interactions and its relationship with mechanical sensitivities and crystal packing, the Hirshfeld surface analysis and the associated 2D-fingerprint plot of these self-assembled energetic materials were also studied [28]. The Hirsfeld surfaces, 2D-fingerprints and interaction contribution plots around the TTDO (or protonated TTDO) in three self-assembled energetic materials are visualized (Fig. 4). The red regions on the Hirshfeld surfaces indicate close contacts, namely strong hydrogen bonds like O…H and N…H interactions. In three crystals, the proportions of these relatively strong hydrogen bonds all surpass 50% (Fig. 4a, b and c right), implying that hydrogen bonds are the main driven force to construct these self-assembled crystals. The 2D-fingerprint results indicate that the hydrogen bond interactions in three crystals are very different. For TTDOH, two spikes representing the interior (left spike, the hydrogen bond acceptor is outside the surface) and exterior (right spike, the hydrogen bond acceptor is inside the surface) O…H interactions are almost the same, indicating that the fuel component (namely neutral TTDO) is almost equally interacted with its adjacent partner and $H_2O_2$ molecules. In contrast, the spikes representing interior O…H interaction are more obvious in TTDON and TTDOP crystals, implying that fuel components (namely protonated TTDO) in TTDON and TTDOP are mainly surrounded by oxidant anions ($NO_3^-$ and $ClO_4^-$) (Fig. 4a, b and c middle). These ubiquitous hydrogen bond networks can act as a buffer against the external mechanical stimulus, consequently their mechanical sensitivities are lower than traditional high explosives with relatively less intermolecular hydrogen bonds (such as RDX and HMX) (Table 1) [29,30]. Despite the proportions of hydrogen bonds are very close for three self-assembled energetic materials, the undesired O-O interactions that generally cause an increase in the mechanical sensitivities of energetic materials in TTDON (11%) and TTDOP (13.2%) are obviously higher than that (3.8%) of TTDOH. Thus, the TTDON (14 J, 196 N) and TTDOP (13 J, 144 N) are more sensitive to TTDOH (> 20 J, > 360 N) under mechanical stimulus. Overall, we have demonstrated that the self-assembly of fuel-rich explosive TTDO with high-energy oxidants is a promising choice to tailor the energy levels and safety properties for the development of intermolecular energetic materials. Accordingly, three novel assembled materials have shown great promise as advanced energetic materials with well-balanced energy and safety.

Moreover, we investigated the thermal stability of TTDO, TTDOH, TTDON and TTDOP by TG/DSC method. From the TG/DSC curves for TTDO, we observed a sharp exothermic peak and an obvious mass loss at 340 °C after a melting endothermic peak at 336 °C which implies the energetic feature of TTDO (Fig. S1). Before the decomposition of TTDO, $H_2O_2$ molecules will first escape from the crystals of TTDOH. Because of the multiple combination modes of $H_2O_2$ molecules in the TTDOH crystals as revealed by its crystal structure, three obvious endothermic peaks were observed at 89 °C, 115 °C, 161 °C, respectively. After the complete escape of $H_2O_2$ molecules from the TTDOH crystals, TTDO decomposed at 311 °C (Fig. S2). For TTDON, the endothermic peak around 137 °C corresponds to the escape of $H_2O$ molecules in the crystals of TTDON and a sharp exothermic peaks and mass loss occurred at 180 °C (Fig. S3). In TTDOP, when the temperature reached 176 °C, TTDOP decomposed instantaneously and an drastic exothermic peak and a mass loss were observed from TG/DSC curves (Fig. S4). Overall, the instantaneous thermal decomposition of these self-assembly energetic material as revealed by their DSC/TG curves indicate their potential applications as promising high explosives.

### 3.3. Combustion and propulsion properties of TTDOP

Due to its high positive $CO_2$-based OB (34%), ammonium perchlorate (AP) is widely used as a high-energy oxidant in solid propellant formulations [31]. But AP also suffers some drawbacks, such as low heat of formation (−295.8 kJ mol$^{-1}$) and specific impulse (157 s, value calculated by Explo5/6.02). In contrast, TTDOP exhibited better comprehensive properties than AP including high density (1.988 g cm$^{-3}$ at room temperature), high heat of formation (714.2 kJ mol$^{-1}$), high specific impulse (284.5 s) and positive $CO_2$-based OB (4.5%). Thus, we think that TTDOP is a promising substitute of AP in solid propellant formulations. So, we utilized high-speed camera (photography operating at 1 kHz) to monitor the combustion behaviors of TTDOP and AP as the high-energy oxidants. All the tested samples were prepared by mixing 300 mg target compounds (TTDOP or AP) with 100 mg powdered aluminium and packed loosely in a burner (Fig. 5a) [32,33].

As shown in Fig. 5b, the combustion of TTDOP-Al mixed sample exhibited a sustainable, stable and violent flame, which was rarely observed for the combustion behaviors of loosely packed sample [34]. However, for the AP-Al mixed sample, no sustainable combustion behaviors were observed and its flame was inconsecutive and less bright (see supplementary video). The total burning duration and burning rate of TTDOP-Al mixed sample were 867 ms and 0.49 m s$^{-1}$, respectively, which were also much superior to those of AP-Al mixed (557 ms and 0.07 m s$^{-1}$, respectively, Fig. 4c). The results of combustion test demonstrated the outstanding combustion behavior of TTDOP as a high-energy oxidant. The excellent combustion performance of TTDOP is

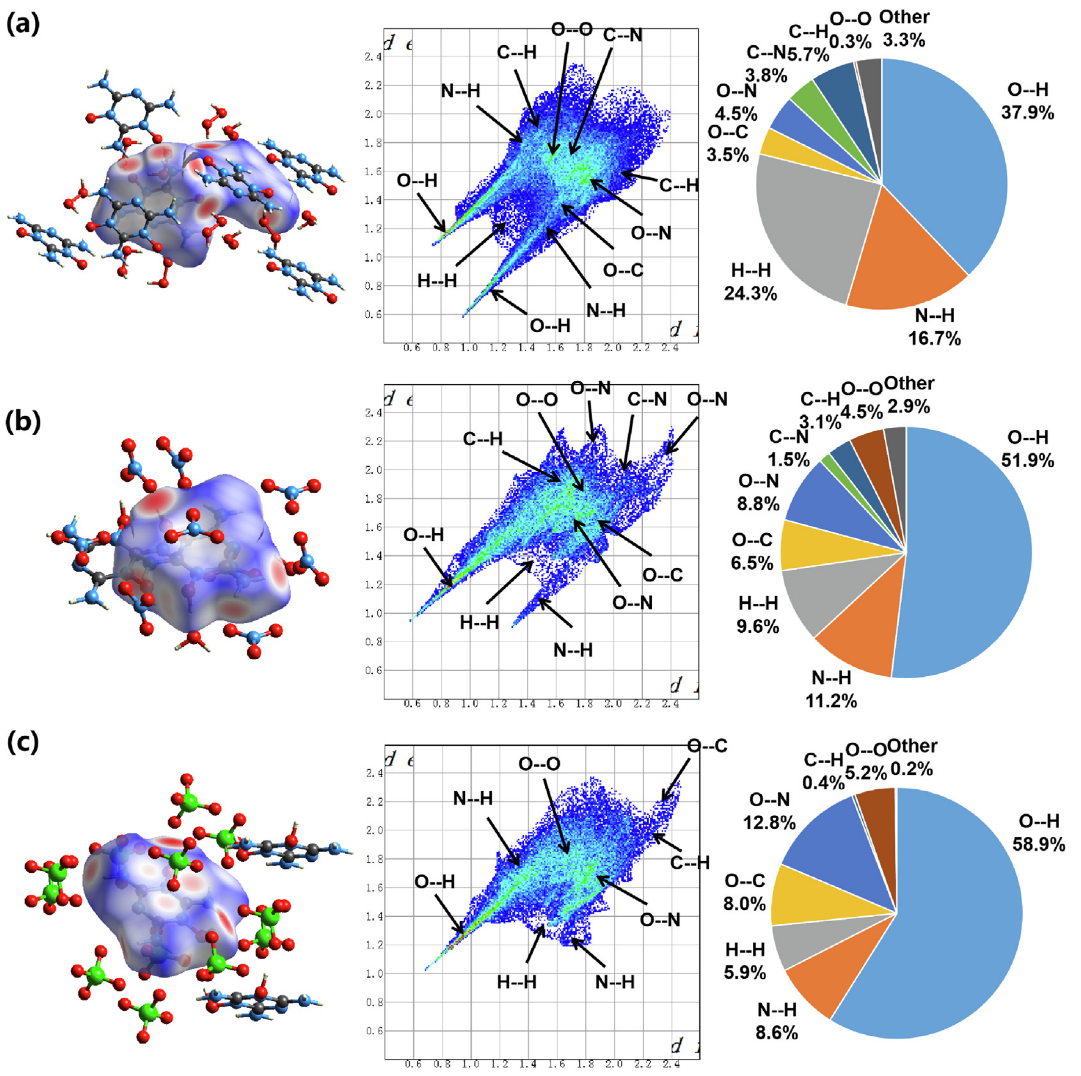

**Fig. 4.** (a) Hirshfeld surfaces, 2D fingerprint plots and the individual atomic contact percentage contribution of TTDOH; (b) Hirshfeld surfaces, 2D fingerprint plots and the individual atomic contact percentage contribution of TTDON; (c) Hirshfeld surfaces, 2D fingerprint plots and the individual atomic contact percentage contribution of TTDOP.

probably due to the high energy of TTDOP, which is very beneficial for generating high temperature oxidizing gas products. These high temperature gas products will tremendously boost the mass and heat transfer, thus the sustainable and violent combustion is observed in the loosely packed sample of TTDOP.

To well evaluate the potential as novel high-energy oxidants in solid propellant formulations, we further calculated the propulsion performances of glycidyl azide polymer (GAP) based propellant formula using TTDOP as a substitution of AP and RDX by EXPLO5 (version 6.02) (Table 2). The basic propellant formulation consists of 10 wt% GAP, 5 wt% Aluminium, 60 wt% AP, and 25 wt% RDX. The specific impulse ($I_{sp}$), characteristic velocity (C*), combustion temperature ($T_c$) and average molecular weight of combustion gas products ($M_c$) are calculated as 2566.6 N s kg$^{-1}$, 1478 m s$^{-1}$, 3360 K and 26.875 g, respectively. As AP was gradually replaced by TTDOP, the energy level of the GAP propellants was elevated in detail. The highest calculated energy parameters were obtained when the content of TTDOP was up to 55 wt %, with the values of 2829.26 N s kg$^{-1}$, 1623 m s$^{-1}$, 3803 K and 23.924, respectively. When AP was totally replaced by TTDOP (a content of 60 wt%), the specific impulse ($I_{sp}$) is up to 2802.80 N s kg$^{-1}$, a little lower than the one (2829.26 N s kg$^{-1}$) of 55 wt% TTDOP. Due to that the detonation properties TTDOP are superior to RDX, we think that further replacing RDX by TTDOP would endow the GAP propellant formulations with higher propulsion capability. Thus, we further increased the content of TTDOP in GAP-based propellant formulations by replacing RDX with TTDOP. As expected, the highest calculated energy parameters of GAP propellants were obtained when the content of TTDOP was increased to 85 wt%, with the values of 2862.58 N s kg$^{-1}$, 1624 m s$^{-1}$, 3955 K and 24.492 g, respectively, whose specific impulse is 11.5% higher than that (2566.62 N s kg$^{-1}$) of the basic GAP propellant formulation. Based on above combustion tests and calculations of propulsion parameters, we think that TTDOP has the great promise as high-energy oxidizer components in the solid propulsion formulations.

## 4. Conclusion

In conclusion, we demonstrated a promising approach of designing explosive-oxidant self-assembled energetic materials by improving proton affinity of explosive precursor. With the direction of ESP and proton affinities calculations, a precursor TTDO was rationally designed and synthesized using melamine as the raw material. Three self-assembled energetic materials (i.e.,TTDOH, TTDON and TTDOP) were readily prepared through intermolecular assembly of TTDO with oxidants ($H_2O_2$, $HNO_3$, $HClO_4$). Their structures and properties were fully characterized. Most impressively, the self-assembled energetic material

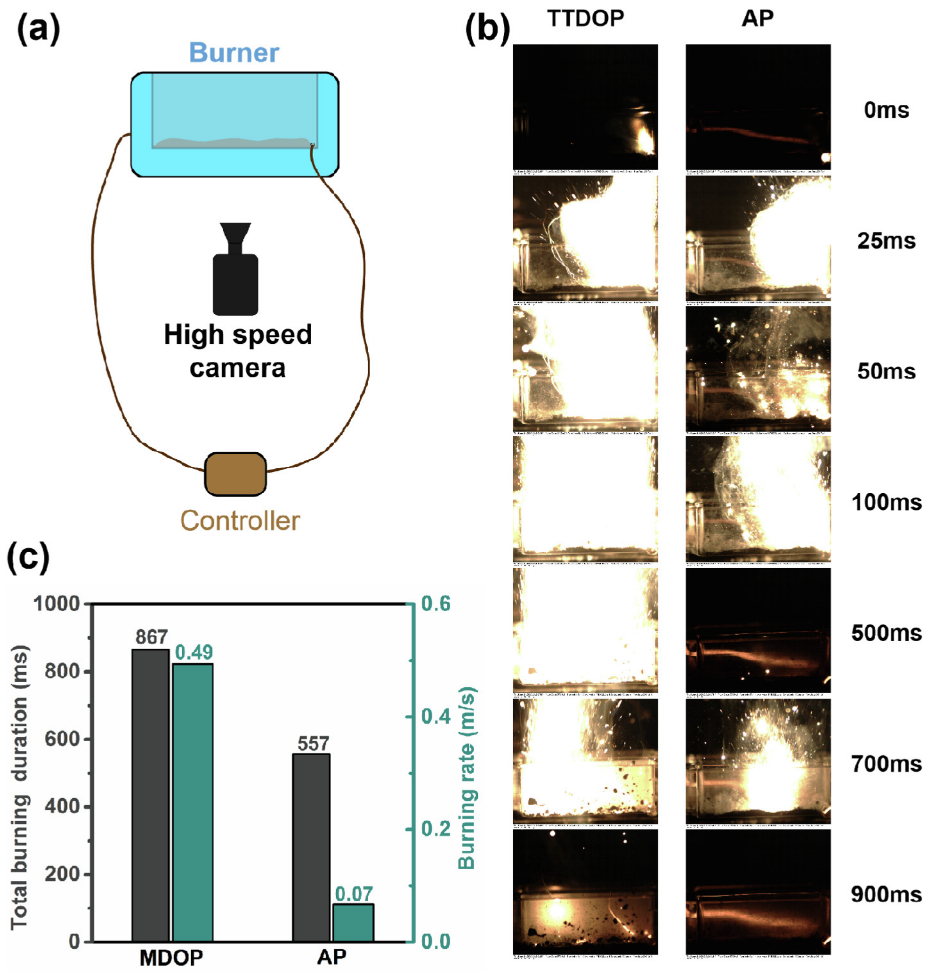

**Fig. 5.** (a) Schematic of combustion test device. (b) Combustion snapshots of TTDOP-Al mixed sample and AP-Al mixed sample. (c) Total burning duration and burning rates of TTDOP-Al mixed sample and AP-Al mixed sample.

TTDOP possesses a high density (2.047 g $cm^{-3}$ at 100 K), detonation properties (9284 m $s^{-1}$ and 41 GPa) comparable to HMX, and meanwhile relatively low mechanical sensitivities (13 J and 144 N). Moreover, the combustion experiments and propulsion property calculations showed that TTDOP has a sustainable and violent combustion behavior (total burning duration 867 ms and burning rate 0.49 m $s^{-1}$) and high specific impulse values (maximum 2862.58 N s $kg^{-1}$, increased by 11.5% compared with original propellant formula), demonstrating its great promise as an AP replacement in solid propellant formulations.

**Table 2**
Propellant performances.

| GAP (%) | Al (%) | AP (%) | RDX (%) | TTDOP (%) | $I_{sp}$ (N s $kg^{-1}$) | C* (m $s^{-1}$) | $T_c$ (K) | Mc (g) |
|---|---|---|---|---|---|---|---|---|
| 10 | 5 | 60 | 25 | 0 | 2566.62 | 1478 | 3360 | 25.879 |
| 10 | 5 | 55 | 25 | 5 | 2592.10 | 1492 | 3410 | 25.703 |
| 10 | 5 | 50 | 25 | 10 | 2615.62 | 1507 | 3456 | 25.523 |
| 10 | 5 | 45 | 25 | 15 | 2640.12 | 1521 | 3500 | 25.338 |
| 10 | 5 | 40 | 25 | 20 | 2662.66 | 1534 | 3542 | 25.153 |
| 10 | 5 | 35 | 25 | 25 | 2691.08 | 1548 | 3583 | 24.968 |
| 10 | 5 | 30 | 25 | 30 | 2704.80 | 1561 | 3622 | 24.784 |
| 10 | 5 | 25 | 25 | 35 | 2744.98 | 1573 | 3660 | 24.603 |
| 10 | 5 | 20 | 25 | 40 | 2769.48 | 1586 | 3696 | 24.426 |
| 10 | 5 | 15 | 25 | 45 | 2771.44 | 1600 | 3733 | 24.252 |
| 10 | 5 | 10 | 25 | 50 | 2779.28 | 1614 | 3768 | 24.085 |
| 10 | 5 | 5 | 25 | 55 | 2829.26 | 1623 | 3803 | 23.924 |
| 10 | 5 | 0 | 25 | 60 | 2802.80 | 1639 | 3837 | 23.773 |
| 10 | 5 | 0 | 20 | 65 | 2840.04 | 1635 | 3864 | 23.924 |
| 10 | 5 | 0 | 15 | 70 | 2847.88 | 1633 | 3890 | 24.072 |
| 10 | 5 | 0 | 10 | 75 | 2853.76 | 1630 | 3913 | 24.215 |
| 10 | 5 | 0 | 5 | 80 | 2858.66 | 1627 | 3935 | 24.355 |
| 10 | 5 | 0 | 0 | 85 | 2862.58 | 1624 | 3955 | 24.492 |

## Declaration of Competing Interest

The authors declare that they have no known competing financial interests or personal relationships that could have appeared to influence the work reported in this paper.

## Acknowledgement

This work was supported by the National Natural Science Foundation of China (No. 21702195, 21875288).

## Appendix A. Supplementary data

Supplementary data to this article can be found online at https://doi.org/10.1016/j.cej.2020.125114.

## References

[1] H. Gao, J.M. Shreeve, Azole-based energetic salts, Chem. Rev. 111 (2011) 7377–7436.

[2] J.P. Agrawal, High Energy Materials: Propellants, Explosives and Pyrotechnics, John Wiley & Sons, 2010.

[3] C. He, J.M. Shreeve, Potassium 4,5-bis(dinitromethyl)furoxanate: a green primary explosive with a positive oxygen balance, Angew. Chem. Int. Ed. 55 (2016) 772–775.

[4] J. Zhang, J.M. Shreeve, 3,3'-dinitroamino-4,4'-azoxyfurazan and its derivatives: an assembly of diverse N-O building blocks for high-performance energetic materials, J. Am. Chem. Soc. 136 (2014) 4437–4445.

[5] M. Göbel, K. Karaghiosoff, T.M. Klapötke, D.G. Piercey, J. Stierstorfer, Nitrotetrazolate-2-oxides and the Strategy of N-Oxide Introduction, J. Am. Chem. Soc. 132 (2010) 17216–17226.

[6] N.R. Greiner, D.S. Phillips, J.D. Johnson, F. Volk, Diamonds in detonation soot, Nature 333 (1988) 440.

[7] M.H.V. Huynh, M.A. Hiskey, D.E. Chavez, D.L. Naud, R.D. Gilardi, Synthesis, characterization, and energetic properties of diazido heteroaromatic high-nitrogen C−N compound, J. Am. Chem. Soc. 127 (2005) 12537–12543.

[8] Q. Yu, P. Yin, J. Zhang, C. He, G.H. Imler, D.A. Parrish, J.M. Shreeve, Pushing the limits of oxygen balance in 1, 3, 4-oxadiazoles, J. Am. Chem. Soc. 139 (2017) 8816–8819.

[9] A.A. Dippold, T.M. Klapötke, A study of dinitro-bis-1,2,4-triazole-1,1′-diol and derivatives: design of high-performance insensitive energetic materials by the introduction of N-oxides, J. Am. Chem. Soc. 135 (2013) 9931–9938.

[10] W. He, P.J. Liu, G.Q. He, M. Gozin, Q.L. Yan, Highly reactive metastable intermixed composites (MICs): preparation and characterization, Adv. Mat. 30 (2018) 1706293.

[11] S.L. Chen, Z.R. Yang, B.J. Wang, Y. Shan, L.Y. Sun, C.T. He, W.X. Zhang, X.M. Chen, Molecular perovskite high-energetic materials, Sci. China Mater. 61 (2018) 1123–1128.

[12] S. Seth, T.P. Vaid, A.J. Matzger, Salt loading in MOFs: solvent-free and solvent-assisted loading of $NH_4NO_3$ and $LiNO_3$ in UiO-66, Dalton Trans. 48 (2019) 13483–13490.

[13] S.L. Chen, Y. Shang, C.T. He, L.Y. Sun, Z.M. Ye, W.X. Zhang, X.M. Chen, Optimizing the oxygen balance by changing the A-site cations in molecular perovskite high-energetic materials, CrystEngComm 20 (2018) 7458–7463.

[14] J.C. Bennion, N. Chowdhury, J.W. Kampf, A.J. Matzger, Hydrogen peroxide solvates of 2, 4, 6, 8, 10, 12-hexanitro-2, 4, 6, 8, 10, 12-hexaazaisowurtzitane, Angew. Chem. Inter. Ed. 55 (2016) 13118–13121.

[15] J. Xu, S. Zheng, S. Huang, Y. Tian, Y. Liu, H. Zhang, J. Sun, Host–guest energetic materials constructed by incorporating oxidizing gas molecules into an organic lattice cavity toward achieving highly-energetic and low-sensitivity performance, Chem. Comm. 55 (2019) 909–912.

[16] Y. Wang, Y. Liu, S. Song, Z. Yang, X. Qi, K. Wang, Q. Zhang, Y. Tian, Accelerating the discovery of insensitive high-energy-density materials by a materials genome approach, Nat. Comm. 9 (2018) 2444.

[17] Y. Wang, S. Song, C. Huang, X. Qi, K. Wang, Y. Liu, Q. Zhang, Hunting for advanced high-energy-density materials with well-balanced energy and safety through an energetic host–guest inclusion strategy, J. Mater. Chem. A 7 (2019) 19248–19257.

[18] J.S. Murray, P. Politzer, The electrostatic potential: an overview, WIRES Comput. Mol. Sci. 1 (2011) 153–163.

[19] P. Politzer, J.S. Murray, The fundamental nature and role of the electrostatic potential in atoms and molecules, Theor. Chem. Acc. 108 (2002) 134–142.

[20] X. Song, J. Li, H. Hou, B. Wang, Extensive theoretical studies of a new energetic material: Tetrazino-tetrazine-tetraoxide (TTTO), J. Comput. Chem. 30 (2009) 1816–1820.

[21] R.V. Kent, R.A. Wiscons, P. Sharon, D. Grinstein, A.A. Frimer, A.J. Matzger, Cocrystal engineering of a high nitrogen energetic material, Cryst. Growth Des. 18 (2017) 219–224.

[22] B.J. Smith, L. Radom, Calculation of proton affinities using the G2 (MP2, SVP) procedure, J. Phys. Chem. 99 (1995) 6468–6471.

[23] M. Sućeska. Explo5 (version 6.02). Zagreb, Croatia, 2013.

[24] B. Chan, J. Deng, L. Radom, G4(MP2)-6X: a cost-effective improvement to G4(MP2), J. Chem. Theory Comput. 7 (2011) 112–120.

[25] D. Tian, F. Zhao, J. Liu, Handbook of Energetic Materials and the Related Compounds, National Defense Industry Press, Beijing, 2011.

[26] Y. Tang, C. He, L.A. Mitchell, D.A. Parrish, J.M. Shreeve, C-N bonded energetic biheterocyclic compounds with good detonation performance and high thermal stability, J. Mater. Chem. A 4 (2016) 3879–3885.

[27] E.C. Koch, Insensitive high explosives II: 3, 3′-diamino-4, 4′-azoxyfurazan (DAAF), Propellants, Explos., Pyrotech. 41 (2016) 526–538.

[28] J.J. McKinnon, M.A. Spackman, A.S. Mitchell, Novel tools for visualizing and exploring intermolecular interactions in molecular crystals, Acta Crystallogr., Sect. B: Struct. Sci. 60 (2004) 627–668.

[29] Y. Ma, A. Zhang, C. Zhang, D. Jiang, Y. Zhu, C. Zhang, Crystal packing of low-sensitivity and high-energy explosives, Cryst. Growth Des. 14 (2014) 4703–4713.

[30] R. Bu, Y. Xiong, X. Wei, H. Li, C. Zhang, Hydrogen Bonding in CHON-Containing Energetic Crystals: A Review, Cryst. Growth Des. 19 (2019) 5981–5997.

[31] Z. Liu, C. Yin, Y. Kong, F. Zhao, Y. Luo, H. Xiang, The thermal decomposition of ammonium perchlorate, Chin. J. Energ. Mater. (Hanneng Cailiao) 8 (2000) 75–79.

[32] W. He, Z. Li, S. Chen, G. Yang, Z. Yang, P. Liu, Q. Yan, Energetic metastable n-Al@PVDF/EMOF composite nanofibers with improved combustion performances, Chem. Eng. J. 383 (2019) 123146.

[33] W. He, P.J. Liu, F. Gong, B. Tao, J. Gu, Z. Yang, Q. Yan, Tuning the reactivity of metastable intermixed composite n-Al/PTFE by polydopamine interfacial control, ACS Appl. Mater. Interfaces 10 (2018) 32849–32858.

[34] V.E. Sanders, B.W. Asay, T.J. Foley, B.C. Tappan, A.N. Pacheco, S.F. Son, Reaction propagation of four nanoscale energetic composites (Al/MoO3, Al/WO3, Al/CuO, and B12O3), J. Propul. Power 23 (2007) 707–714.